Is ISAR Interferometry Able to Detect Slope Deformations of Open Pit Mines?

Andrew Jarosz and Luke Shepherd
Curtin University, Western Australian School of Mines, Mine Surveying Program

ABSTRACT: The satellite based Synthetic Aperture Radar Interferometry (InSAR) system has the capacity to detect vertical movements of ground surface with sub-centimetre accuracy. Reports of current research, on the use of InSAR technology for monitoring seismic events such as earthquakes and ice motion, validate the application of InSAR for the determination of mining induced surface deformation. Most investigations confirm high reliability of results from satellite interferometry. The climate conditions of Western Australia (dry, cloudless weather, minimal rainfalls) are conducive to provide very reliable InSAR interferograms. It is hoped that this technology can be applied for monitoring of surface deformations, especially in a vicinity of open pit slopes, indicating their stability. This paper presents the initial results of the research project carried by WASM Mine Surveying Program and supported by the WA mining industry and European Space Agency (ESA, Project Category 1).

1 INTRODUCTION

Surface deformations and slope stability are very important issues to the mining industry. Slope and batter instability can be a potential source of danger for people and equipment. It may also disrupt mine scheduling and increase the cost of mining production (Lilly *et al*., 2000; Kido *et al*., 2000; Bromhead, 1992). Surface subsidence, that occur above underground mining and in areas adjacent to open pit operations, may affect buildings and other man made structures. The effective prediction and management of mining induced deformations of ground surface should be a key concern for the mining industry.

Existing stability monitoring systems in open pit mining can be divided into two categories, namely, surveying techniques and geotechnical methods (Ding *et al*., 1998; Thompson *et al*., 1993; Bromhead, 1992).

Surveying techniques can be used to determine the absolute positions and positional changes of any point on the surface. When using survey techniques, survey instruments such as levels, theodolites, total stations, GPS receivers and photogrammetric cameras are usually utilised to collect data. Surface deformation monitoring systems employ a levelling line or mesh of points to establish vertical movement. Currently, highly accurate total stations and GPS systems are favoured for there ability to determine all three spatial coordinates (X, Y, Z). Post-processing techniques can determine the positions of surveyed targets, in relation to a stable references, and further, determine their movements by comparing positions from at least two different surveys.

Geotechnical monitoring methods usually employ specialised instrumentation to measure deformation or displacement over a relatively short measurement range. Common geotechnical instrumentations used in slope stability deformation surveys include (Ding *et al*., 1998; Logan *et al*., 1993; Loubser, 1993): crack measuring pins, extensometers, inclinometers, piezometers, tilt-meters and microseismic geophones.

Surveying and geotechnical monitoring systems are usually established in areas where the likelihood of deformation is very high. The main advantage of the conventional monitoring

techniques used for deformation control is the high accuracy of measurements. However, the major disadvantages are complicated instrumentation, small number of observations, and high cost of frequent surveys.

In the resent years the satellite based remote sensing technologies have been utilised for deformation monitoring. Of the special interest is the method employing a space borne Synthetic Aperture Radar (SAR) system. This method combined with comparative processing of space radar scans (InSAR) is able to detect relatively small movements (of sub-centimetre magnitude) occurring on the earth's surface. So far the method was utilized to monitor a large-scale geomorphological processes, earthquakes, volcanic eruptions and deformation and glacier movements. Initial research was conducted, to utilize this method to monitor vertical deformations in coalfield areas. At the start of this year the Mine Surveying Program at WASM initiated a research project that investigates the applicability of the Synthetic Aperture Radar Interferometry (InSAR) to determine surface deformations induced by open pit mining operations. Implementing differential interferometry to monitor mining deformations could increase the safety margins in mining operations. Monitoring of changes in pit depths, heights of stockpiles and waste dumps, and levels of tailing storage facilities may provide additional important production data.

2 BACKGROUND OF INSAR TECHNOLOGY

Synthetic Aperture Radar System

Spaceborne Synthetic Aperture Radar (SAR) utilizes the following components and principles (Raney, 1998; Olmsted, 1993):

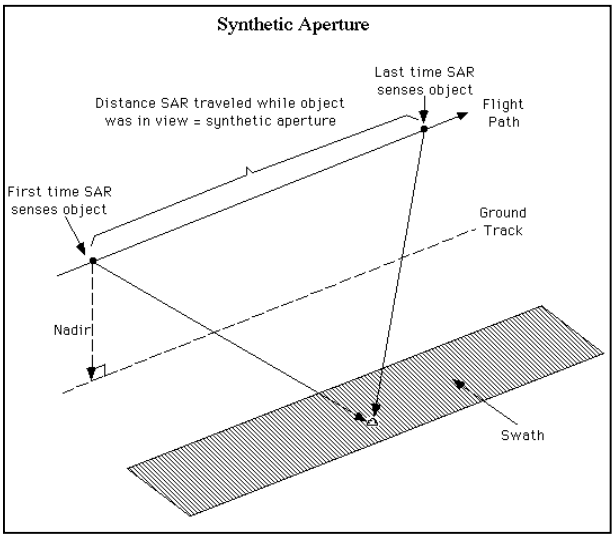

Figure 1: Synthetic Aperture Radar set up (after Alaska Sar Facility, 2001)

- An antenna that emits a short electromagnetic (radar) pulses in a specific direction,
- A receiving antenna that detect the backscattered signal with directional precision,
- A clock that measures the time delay between emission and detection,
- A scanning system that allows to scan the surface of the earth with the directional beam and to determine a direction and range to a target.

In general, the directional antenna generates a radar backscatter map by scanning the surface of the Earth moving at uniform speed and altitude along the flightpath. The sensor moves along the satellite flightpath and transmits microwave pulses and then receives the echoes of this pulse via the same antenna. The SAR sensor is known as an active radar sensor. To increase image quality, the SAR system uses spacecraft movement and advanced signal processing techniques to simulate a larger sensor size (Fig. 1 – after Alaska SAR Facility, 2001). The spot on the Earth that is illuminated by a single pulse is referred to as the antenna footprint while the imaged strip on the ground is called the swath (Bamler, 1993; Campbell, 1996) (Fig. 2). For example, the ERS-1 satellite sends out approximately 1700 pulses a second and collects approximately one thousand backscattered responses from a single object.

The real backscattered returned signal is estimated near the centre of the beam by detecting Doppler Frequency Shifts and filtered using Fast Furrier Transformation (*FFT*) function (Franceschetti, *et al*., 1999; Gonzalez, *et al*., 1993; Gilbert, 1986). Doppler Shift is a change in

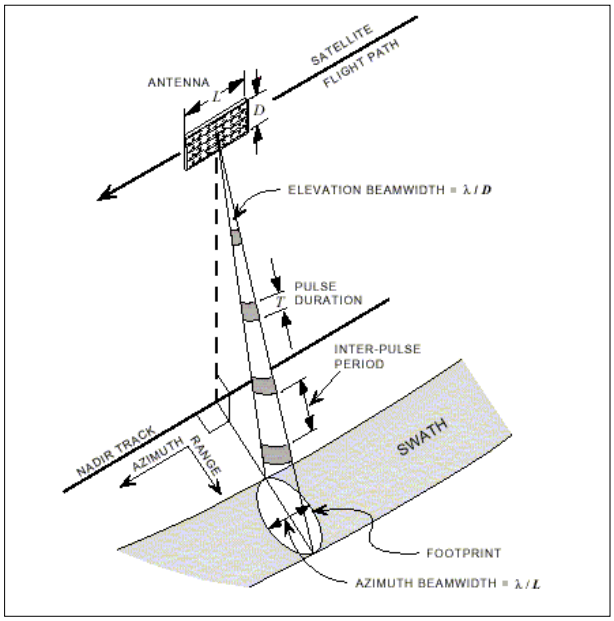

Figure 2: Imaging geometry of a space-borne SAR system /ERS-1 configuration/ (after Olmsted, 1993)

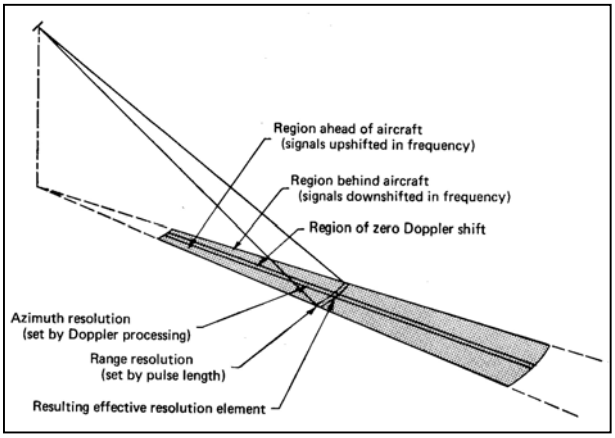

Figure 3: Determination of resolution in SAR system (after Franceschetti, G, et al., 1999)

wave frequency as a function of the relative velocities of a transmitter and a reflector. In practise this means that the signal returned from the area ahead of the spaceborne sensor has an upshifted (higher) frequency. Conversely, the signal from the area behind the sensor has a downshifted (lower) frequency. By processing the returned signal using the Doppler Shift, a very small effective beamwidth (Fig. 3) is obtained. Thus, the resolution of a synthetic SAR system depends on the size of the antenna but is independent of the orbital height (Lillesand *et al*., 2000; Franceschetti, *et al*., 1999; Olmsted, 1993; Mensa, 1991; Fitch 1988). The SAR system provides high quality images of the Earth through post-processing of raw signal data. The quality of the image depends on the sensor-scene geometry and signal processing. There are two fundamental characteristics of the system. The first is the *spatial resolution of the image* in which the azimuth resolution is independent of the range but the range resolution is linked to the position on the image. In other words, the pulse duration determines range resolution. The second is the *point spread function* (PSF), which determines the correlation and sampling properties of the image (Oliver *et al*., 1998; Rihaczek *et al*., 1996; Hovanessian, 1980; Lybanon, 1973).

In practice, a radar image is composed of many dots (pixels). Each pixel in the radar image represents the radar backscatter for the corresponding area of the ground surface. Dark areas in the image represent low backscatter while bright areas represent a high backscatter signal.

Differential Interferometry

Differential Interferometry exploits the coherent nature of SAR echoes to measure the difference in phase of the backscattered signal. If the position of the antennas are known accurately and if the same object can be scanned from the same location at two different times then the difference in the backscattered signal's phase infer object movement. Similarly, if the phase difference is obtained when the same object is scanned from two locations, the height of the object can be established. The inpath length differences are a function of the topography of the surface, changes in the position of targets on the Earth and the differences in atmospheric or ionospheric conditions. The differential interferometry technique use two or more observations, made from approximately the same location in space (distance between two positions of the sensor, called a baseline, should be minimum) at different times (Plaut, *et al*., 1999; ESA

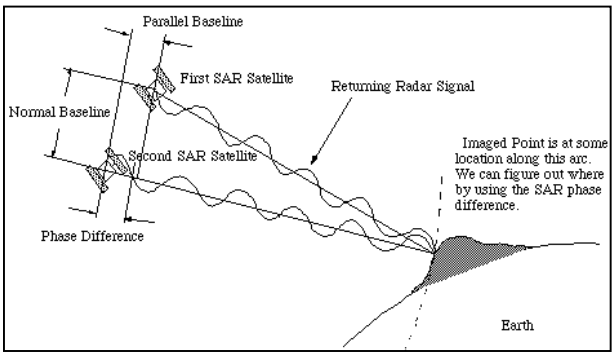

Figure 4: Interferometry set up /after Alaska SAR Facility, 2001/

Service, 2001). After removing the topographic and orbital components the ground movements along the line of sight between the radar and the target are obtained. Any displacement of the scene appears directly as a phase shift with respect to the rest of the scene. In other words, the radar measures scalar change in the satellite-ground distance (Fig. 4). For example, if the ground target moves along the radar-viewing axis by half a wavelength, it will be seen as one fringe in the interferogram, which equals 28 mm for ERS-1 and ERS-2 systems (ESA Service, 2001).

InSAR Data Processing

The interferogram is defined as the product of the complex value of a slave image and the complex conjugate of a master image (Alaska SAR Facility, 2001). By subtracting the phase of two-registered Side-Look Complex (SLC) SAR data images, pixel by pixel, an interferogram can be produced. The size of one pixel may vary from 8 m to 40 m depending on a satellite and SAR system. The SLC images represent SAR data after pre-processing; however, they retain every sample as complex data. Phase continuity information is also preserved within the image. The amplitudes of the corresponding pixels are averaged and the difference of phase values is calculated for each point of the image. The phase difference is given in the range from $-\pi$ to π, called modulo 2π, and is colour encoded as fringes (ESA Service, 2001; Alaska SAR Facility, 2001; Kampes, B., 1999; Franceschetti, *et al*., 1999; Massonnet, 1993).

In the SAR system, the phase of the backscattered signal is compared to a reference wave. The phase of a SAR image is actually the phase difference between the backscattered signal and the reference signal. This phase difference is the result of path length between target and sensor, which can be determined by elevation difference, atmosphere, noise and deformation (Alaska SAR Facility, 2001; Ghiglia, 1998).

The deformation of the range is based on the principle that the difference of the phase is proportional to the range distance. This is the case until the signals have a fixed relation in phase ie the signal is coherent. The coherence is measure of the correlation between the phase information of two corresponding signals. The degree of coherence can be used as a measure of quality (Alaska SAR Facility, 2001; Ghiglia, 1998).

Several sources of errors listed below can lead to a complete loss of phase coherence (Alaska SAR Facility, 2001; ESA Service, 2001):

Thermal noise,
Phase errors due to the processing,
Slightly different viewing positions,
Change in the object phase between acquisitions,
Different atmospheric conditions between acquisitions,
Extremely long perpendicular baselines.

The phase information included in the interferogram is directly related to the topography and is given modulo 2π. To calculate the elevation of each point, the integer number of the phase cycles needs to be added to each phase measurement. This gives the correct slant range distance. This process is referred to as phase unwrapping. The final stage is to take the unwrapped phase information, containing the topographic information, and convert it to a digital elevation model (DEM) (Ghiglia, 1998; Massonnet, 1993).

By producing, analysing and validating the differential interferogram, the ground deformation can be determined. A differential interferogram can be generated from two or more SAR images (SLC) depending on the type of method used. There are two methods used to produce a differential interferogram. The first method is based on three sets of SAR data (three SLC images are required).

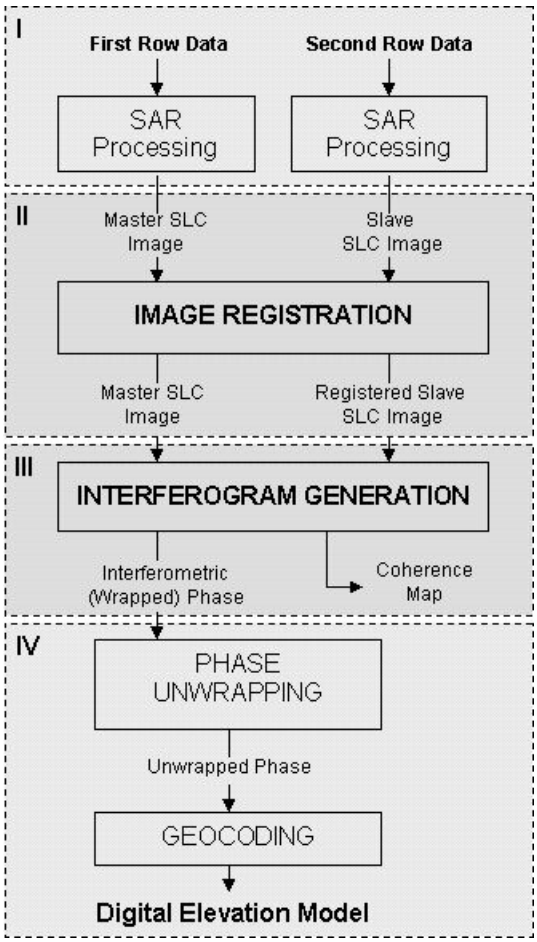

Figure 5: Block diagram of InSAR processor (after Franceschetti, 1999)

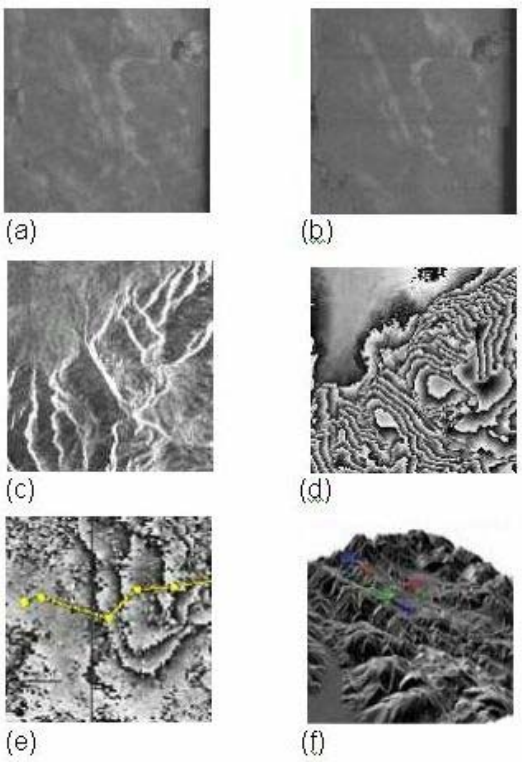

Figure 6: Example of data and InSAR products. (a, b) – SLC images (after ESA, 2001); (c) - SAR amplitude (after Alaska SAR Facility, 2001); (d) - phase difference (after Alaska SAR Facility, 2001); (e) – interferogram of deformation (after NPA Group, 2001); (f) - DEM (after ESA, 2001)

The method removes the topographic contribution from an interferogram containing topography, deformation and atmospheric components (Kampes, B., 1999). Any deformation can be then obtained by a calculation process taking into account two unwrapped interferograms (Alaska SAR Facility, 2001).

The second method is based on an existing DEM, which can be registered to the geometry of the calculated interferogram from two SLC images. The result is a simulated interferogram. The difference of the original and simulated interferogram is the required differential interferogram (Alaska SAR Facility, 2001; Franceschetti, *et al*., 1999; Plaut *et al*., 1999). Finally to compare interferometric products with other sources (maps), the geocoding process is required to project an interferogram to a common reference system.

The entire InSAR process is outline in Figure 5 (Franceschetti, *et al*., 1999; Kampes, B., 1999). The first block (I) depicts the processing and transformation of row data (radar and orbital) into, for instance, a Single Look Complex image format. This first step of the InSAR processing is performed by ESA before distribution of SLC images. The second block (II) consists of registration, where the slave image is aligned with the master image, and the

computation of the reference phase of the ellipsoid is performed. Because the slave image is acquired from a different viewing point than the master (reference) image, the data must be re-sampled before the slave image can be projected onto the first master image (ESA Service, 200; Kampes, B., 1999). In this step, the offset vectors of the alignment of the slave image to the master image are estimated by computing the correlation of the magnitude images for shifts and pixel levels. Based on the estimated vectors, the 2d-polynomial model of required degree of correlation is computed. The least square method is used to determine the final solution (Doris, 2001). In the third block (III), the interferometric phase image and the coherence maps are computed. Finally, in the fourth block (IV), DEM and deformation maps are created.

3 MINING APPLICATIONS OF INSAR

The modern open pit and underground mining operations usually have significant area of extent. They can also influence relatively large portions of terrain adjacent to the crest of an open pit or above longwall or room-and-pillar extraction areas. The significant extent of mining operations is an important factor that suggests that InSAR based subsidence monitoring techniques may be applicable.

Initial research efforts have focused on the application of InSAR for monitoring of mining induced subsidence over the coalfields (Stow *et al*., 1995, Perski *et al*., 2000). The research suggests that the method can produce valuable and accurate results. In the report by R. Stow *et al*. (1995) authors conclude, "… Mining subsidence can be detected using 35 day repeat SAR data and SAR interferometry techniques, and that this subsidence can be measured at the very least to an accuracy of few centimetres. However, there would appear to be a central dilemma in applying this technique. A balance needs to be found between a usable temporal separation between images (in terms of interferogram coherence) and allowing a suitable length of time to lapse for measurable amount of subsidence to occur."

Taking the above into account and very favourable weather and ground conditions of Western Australia, it seems reasonable to assume that InSAR technology may be successfully used for deformation (subsidence) monitoring in the vicinity of large open pit mining operations (Fig.7). The results of InSAR processing may indicate early ground movement of pit walls and prompt more detailed monitoring (using classical surveying methods) or other actions preventing lose of life and equipment due to wall failure.

Figure 7: Large surface deformations next to an open pit mine.

4 SLOPE STABILITY MONITORING USING INSAR – RESEARCH PROJECT

At the start of 2002 the Mine Surveying Program of WASM (Curtin University) was able to obtain some industrial support for "pre-feasibility" study focused on application of InSAR for monitoring of subsidence in the vicinity of large open pit operations. The project also gained support from European Space Agency (ESA) and is classified as a Project Category 1, that provides discounted prices for satellite radar imaginary. At present, three test sites have been chosen for initial InSAR processing. The primary focus of research will be the Leinster (WA) site with further studies at Kalgoorlie (WA) and Eastern Pilbara region (optional).

The selection of the primary test site was determined by the existence of large-scale surface deformations in the proximity of open pit. It is believed that large surface deformations (subsidence) are caused by underground extraction (using a sublevel caving method) of an ore-body that has followed the open pit phase of mining. Also, an important factor in choosing the test site is the availability of deformation monitoring data that has been collected using classical survey and GPS methods. Existence of such data will provide a reference base for assessment of results obtained from InSAR.

After reviewing the available software for InSAR processing it was decided that DORIS InSAR Processor (Kempes *et al*., 1999) is to be used in the initial phase of this project. DORIS is free software (for non-commercial scientific purpose) that runs on UNIX/Linux OS. It can generate interferometric products and end-products from Single Look Complex data provided by ERS1 and ERS2 ESA satellites.

A search of an ESA On-Line Catalogue (EOLI from http://odisseo.esrin.esa.it/) for available interferometry data for the Leinster region produced the following results that could be used for this project.

Table 1.

No.	Frame	Orbit	Baseline	Satellite	Date
1	4164	22650	0	ERS1	1995-11-14
2	4164	2977	515	ERS2	1995-11-15
3	4164	8488	318	ERS2	1996-12-04
4	4164	9991	-199	ERS2	1997-03-19
5	4164	34039	?	ERS2	2001-10-24
6	4164	35041	630	ERS2	2002-01-02

The usefulness of data was determined on the bases of date (in relation to development of deformations), satellite baseline and weather conditions.

Up to the date ESA provided data (ERS SLC cdroms) that included one tandem pair from November 1995 and one 490 day repeat. The available data sets (No. 1, 2 and 4) were used for processing and are bases for the presented preliminary results.

5 PRELIMINARY RESULTS AND FUTURE DIRECTIONS

The tandem pair of ERS SLC satellite radar images from 14/15 November 1995 with a base of 515 m was used to generate the reference interferogram that includes topographical effects only. It is assumed that it does not include any effects of deformations as the underground mining had just started.

The 490 day repeat interferogram was generated using data from 14-November-1995 and 19-March-1997 with a baseline of -199 m. A small section of the interferogram is presented in Figure 7. The presented area is limited to the vicinity of Leinster mining operation. The data were filtered and multi-look processed to improve phase statistics. The interferogram has horizontal resolution at the ground level of about 20 m.

The initial review of the results suggests very good coherency between both SLC images despite the very long time base (490 days). This suggests that Western Australian conditions are ideal for long-term interferometry analysis and the InSAR technology should be able to detect the long-term and slow ground movements.

The interferogram, itself, does not yield any conclusive results, as there was minimal subsidence movement during the investigated period. Underground mining was initiated at the end of 1996 and any meaningful subsidence results were detected (using classical surveying methods) in the second half of 1997. The analysis of recent SLC radar images, ordered from ESA (No. 5 and 6), should prove the existence of deformations.

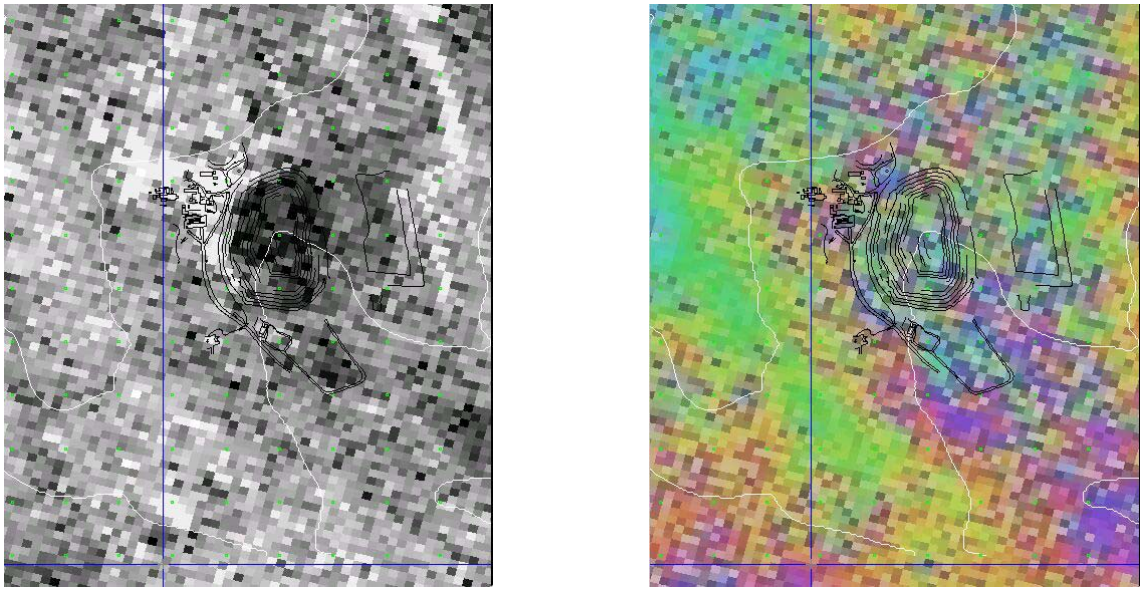

a) Coherence b) Interferogram (with topo)

Figure 8: Interferogram of Leinster area.

6 ACKNOWLEDGMENTS

A portion of this paper is based on the research proposal ***"Application of Satellite Radar Interferometry for Deformation Surveys in the Australian Mineral Industry"*** prepared, in April 2001 under the supervision of Dr A. Jarosz, by Mr I. Baran as his Application for his Candidacy (Post-graduate studies at WASM).

The European Space Agency's (ESA) ERS-1 and ERS-2 satellite(s) have been used to collect the interferometry data. The data were obtained as a part of ESA Cat-1 Project (No.1123).

The interferometry processing in this project was performed using the freely available Doris software, developed by the Delft Institute for Earth-Oriented Space Research (DEOS), Delft University of Technology (http://www.geo.tudelft.nl/doris.html) and the demo version of EarthView software (EV-InSAR v2.0.2) from Atlantis Scientific Inc., Canada (http://www.atlsci.ca/).

7 REFERENCES

Alaska SAR Facility: The Alaska Sar Facility Home Page, [Online], 2001, Available: http://www.asf.alaska.edu [2001, March 31].

Bamler, R., Schättler, B., (1993) SAR Geocoding: *Data and Systems*, Schreier, G., (ed.), Wichmann, Karlsruhe, Germany, pp. 53-102.

Bromhead, E. N., (1992) The Stability of Slopes, Blackie Academic & Professional, 2 ed., London, UK, pp. 1-377.

Campbell, J.B., (1996) Introduction to Remote Sensing, 2 ed., The Guilford Press, New York, USA, pp. 201-238.

Ding, X., Montgomery, S. B., Tsakiri, M., Swindells, C. F. and Jewell, R. J., (1998) Integrated Monitoring Systems for Open Pit Wall Deformation, Australian Centre for Geomechanics, ACG: 1005-98, Meriwa Report No. 186, Perth, Australia, pp. 3-114.

Doris InSAR Processor: Delft object-oriented radar interferometric software, [Online], 2001, Available: http://www.geo.tudelft.nl/fmr/research/insar/sw/doris/index.html.cgi [2001, March 31].

ESA Service: ERS Mission Home Page, [Online], 2001, Available: http://erth.esa.int [2001, March 31].

Fitch, J.P., (1988) Synthetic Aperture Radar, Springer-Verlag, New York, USA, pp. 1-83.

Franceschetti, G., Lanari, R., (1999) Synthetic Aperture Radar Processing, CRS Press, New York, USA, pp.1-284.

Ghiglia, D. C., Pritt, M.D., (1998) Two-Dimensional Phase Unwrapping, *Theory, Algorithms, and Software*, John Wiley & Sons, Inc., New York, USA, pp.1-310.

Gilbert, S., (1986) Introduction to Applied Mathematics, Wellesley-Cambridge Press, Wellesley, USA, pp. 264-366.

Gonzalez R. C., Woods R. E., (1993) Digital Image Processing, Addison-Wesley Publishing, Inc, New York, USA, pp. 81-159.

Hovanessian, S. A., (1980) Synthetic Array and Imaging Radars, Artech House, Washington, USA, pp. 1-30.

Kido, K., Yoshinaka, R., Hagiwara, K. and Sasaki, K., (2000) Stability Analysis and Deformation Behavior of Large Excavated Rock Slopes*, An International Conference on Geotechnical & Geological Engineering*, Melbourne, Australia, [CD-ROM], pages unavailable.

Kampes B. and Usai, S., (1999) Doris: the Delft Object-oriented Radar Interferometric Software. In *2nd International Symposium on Operationalization of Remote Sensing,* Enschede, The Netherlands, 16-20 August, 1999.

Kampes, B., (1999) Delft Object-oriented Radar Interferometric Software User's manual, Delft University of Technology, Nederlanden.

Logan, A. S., Villaescusa, E., Stampton V. R., Struthers, M. A. and Bloss, M. l., (1993) Geotechnical Instrumentation and Ground Behaviour Monitoring at Mount Isa, Geotechnical Instrumentation and Monitoring in Open Pit and Underground Mining, Szwedzicki, T. (ed.), A. A. Balkema, Rotterdam, Netherlands, pp. 321-329.

Loubser, P., (1993) Detection of Abandoned Mine Workings at KCGM's Open Pit Operations, Geotechnical Instrumentation and Monitoring in Open Pit and Underground Mining, Szwedzicki, T. (ed.), A. A. Balkema, Rotterdam, Netherlands, pp. 331-338.

Lillesand, T. M., Kiefer R. W., (2000) Remote Sensing and Image Interpretation, 4 ed., John Wiley & Sons, Inc., New York, USA.

Lilly, P., Xu, D. and Walker, P., (2000) Stability and Risk Assessment of Pit Walls at GHP Iron Ore's Mt Whaleback Mine*, An International Conference on Geotechnical & Geological Engineering*, Melbourne, Australia, [CD-ROM], pages unavailable.

Lybanon, L., (1973) Processing for Spaceborne Synthetic aperture Radar Imagery, *NASA contractor report*, NASA CR-2193, Computer Sciences Corporation, Washington DC, USA, pp. 3-28.

Massonnet, D., (1993) SAR Geocoding: *Data and Systems*, Schreier, G., (ed.), Wichmann, Karlsruhe, Germany, pp. 397-415.

Mensa, D.L., (1991) High Resolution Radar Cross-Section Imaging, Artech House, Boston, USA, pp. 7-41.

Oliver, Ch., Quegan, S., (1998) Understanding Synthetic Aperture Radar Images, Artech House, Boston, USA, pp.11-121.

Olmsted, C., (1993) Scientific SAR User's Guide, Alaska SAR Facility, internal document, Fairbanks, Alaska, pp. 1-34.

Perski, Z., Krawczyk, A., (2000) Application of Satellite Radar Interferometry on the Areas of Underground Exploitation of Copper ore in LGOM – Poland, 11th International Congress of the International Society for Mine Surveying, Krakow, Poland, Vol.2, pp. 209-218.

Plaut, J. J., Rivard, B. and D'lorio, M. A., (1999) Remote Sensing for the Earth Sciences: *Manual of Remote Sensing*, 3 ed., Vol.3, Rencz, N. A. (ed.), John Wiley & Sons, Inc., New York, USA, pp. 613-642.

Raney, R. K., (1998) Principles and Applications of Imaging Radar: *Manual of Remote Sensing*, 3 ed., Vol. 2, Henderson F. M. and Levis, A. J. (ed.), John Wiley & Sons, Inc., New York, USA, pp. 10-21.

Rihaczek, A. W., Hershkowitz, S. J., (1996) Radar Resolution and Complex-Image Analysis, Artech House, Inc, Boston, USA, pp. 71-86

Stow, R. J., Wright P., (1997) Mining Subsidence Land Surveying by SAR Interferometry, 3rd ERS SYMPOSIUM Florence 97 - Abstracts and Papers, Available: http://earth.esa.int/symposia//papers/ [2002, June 30].

Thompson, P. W., Cierlitza, S., (1993) Identification of a Slope Failure Over a Year before Final Collapse Using Multiple Monitoring Methods, Geotechnical Instrumentation and Monitoring in Open Pit and Underground Mining, Szwedzicki, T. (ed.), A. A. Balkema, Rotterdam, Netherlands, pp. 491-511.